6. Quadt, R., Collett, M. & Walls, D. F. Measurement of atomic motion in a standing light field by homodyne detection. *Phys. Rev. Lett.* **74,** 351–354 (1995).
7. Mabuchi, H., Turchette, Q. A., Chapman, M. S. & Kimble, H. J. Real-time detection of individual atoms falling through a high-finesse optical cavity. *Opt. Lett.* **21,** 1393–1395 (1996).
8. Münstermann, P., Fischer, T., Pinkse, P. W. H. & Rempe, G. Single slow atoms from an atomic fountain observed in a high-finesse optical cavity. *Opt. Commun.* **159,** 63–67 (1999).
9. Mabuchi, H., Ye, J. & Kimble, H. J. Full observation of single-atom dynamics in cavity QED. *Appl. Phys. B* **68,** 1095–1108 (1999).
10. Hu, Z. & Kimble, H. J. Observation of a single atom in a magneto-optical trap. *Opt. Lett.* **19,** 1888 (1994).
11. Ruschewitz, F., Bettermann, D., Peng, J. L. & Ertmer, W. Statistical investigations on single trapped neutral atoms. *Europhys. Lett.* **34,** 651–656 (1996).
12. Haubrich, D. *et al.* Observation of individual neutral atoms in magnetic and magneto-optical traps. *Europhys. Lett.* **34,** 663–668 (1996).
13. Neuhauser, W., Hohenstatt, M., Toschek, P. E. & Dehmelt, H. Localized visible Ba^+ mono-ion oscillator. *Phys. Rev. A* **22,** 1137–1140 (1980).
14. Wineland, D. J. & Itano, W. M. Spectroscopy of a single Mg^+ ion. *Phys. Lett. A* **82,** 75–78 (1981).
15. Ye, Y., Vernooy, D. W. & Kimble, H. J. Trapping of single atoms in cavity QED. *Phys. Rev. Lett.* **83,** 4987–4990 (1999).
16. Berman, P. R. (ed.) *Cavity Quantum Electrodynamics* (Academic, San Diego, 1994).
17. Horak, P., Hechenblaikner, G., Gheri, K. M., Stecher, H. & Ritsch, H. Cavity-induced atom cooling in the strong coupling regime. *Phys. Rev. Lett.* **79,** 4974–4977 (1997).
18. Hechenblaikner, G., Gangl, M., Horak, P. & Ritsch, H. Cooling an atom in a weakly driven high-Q cavity. *Phys. Rev. A* **58,** 3030–3042 (1998).
19. Carmichael, H. *An Open Systems Approach to Quantum Optics* (Springer, Berlin, 1993).
20. Mølmer, K., Castin, Y. & Dalibard, J. Monte Carlo wave-function method in quantum optics. *J. Opt. Soc. Am. B* **10,** 524–538 (1993).
21. Mancini, S., Vitali, D. & Tombesi, P. Stochastic phase space localization for a single trapped particle. *Phys. Rev. A* (in the press).
22. Cirac, J. I., Zoller, P., Kimble, H. J. & Mabuchi, H. Quantum state transfer and entanglement distribution among distant nodes in a quantum network. *Phys. Rev. Lett.* **78,** 3221–3224 (1997).
23. Law, C. K. & Eberly, J. H. Arbitrary control of a quantum electromagnetic field. *Phys. Rev. Lett.* **76,** 1055–1058 (1996).
24. Law, C. K. & Kimble, H. J. Deterministic generation of a bit-stream of single-photon pulses. *J. Mod. Opt.* **44,** 2067–2074 (1997).
25. Kuhn, A., Hennrich, M., Bondo, T. & Rempe, G. Controlled generation of single photons from a strongly coupled atom-cavity system. *Appl. Phys. B* **69,** 373–377 (1999).

Acknowledgements

We thank P. Münstermann for important contributions to the experiment. The experiments were performed at the University of Konstanz. Funding by the Deutsche Forschungsgemeinschaft, the Optikzentrum Konstanz and the TMR network 'Microlasers and Cavity QED' is gratefully acknowledged.

Correspondence and requests for materials should be addressed to G. R. (e-mail: Gerhard.Rempe@mpq.mpg.de).

An algorithmic benchmark for quantum information processing

E. Knill*, R. Laflamme*, R. Martinez* & C.-H. Tseng†

* *Los Alamos National Laboratory, MS B265, Los Alamos, New Mexico 87545, USA*

† *Department of Nuclear Engineering, MIT, Cambridge, Massachusetts 02139, USA*

Quantum information processing offers potentially great advantages over classical information processing, both for efficient algorithms[1,2] and for secure communication[3,4]. Therefore, it is important to establish that scalable control of a large number of quantum bits (qubits) can be achieved in practice. There are a rapidly growing number of proposed device technologies[5–11] for quantum information processing. Of these technologies, those exploiting nuclear magnetic resonance (NMR) have been the first to demonstrate non-trivial quantum algorithms with small numbers of qubits[12–16]. To compare different physical realizations of quantum information processors, it is necessary to establish benchmark experiments that are independent of the underlying physical system, and that demonstrate reliable and coherent control of a reasonable number of qubits. Here we report an experimental realization of an algorithmic benchmark using an NMR technique that involves coherent manipulation of seven qubits. Moreover, our experimental procedure can be used as a reliable and efficient method for creating a standard pseudopure state, the first step for implementing traditional quantum algorithms in liquid state NMR systems. The benchmark and the techniques can be adapted for use with other proposed quantum devices.

In NMR experiments the qubits are given by coupled spin-half nuclei in a molecule[9,10]. A large number of identical molecules are dissolved in a liquid and used as an ensemble of quantum registers. Control is by radio frequency (r.f.) pulses. The initial state is the thermal state and the readout is an ensemble measurement using standard NMR methods. By preparing pseudopure states, it is possible to benchmark quantum algorithms involving up to about ten qubits to determine how reliable the available control methods are. There have been numerous NMR experiments implementing various quantum algorithms[12–15]. The benchmark proposed and implemented here with seven nuclei requires generating a 'cat state' and then decoding it to the standard initial state. For qubits implemented by spins, the standard initial state has all spins down. The cat state consists of an equal superposition of two states: one with all spins up and the other with all spins down. The cat state is among the most fragile states that are used by quantum computers. A high fidelity realization of our benchmark therefore demonstrates excellent coherent control over the system of qubits.

To simplify the discussion, we use a three-qubit example of the cat-state benchmark. We use deviation density matrices[17] for describing states of the nuclei. This means that states are described by the traceless part of the density matrix up to an overall scale. The thermal equilibrium state of a molecule with one proton (H) and two ^{13}C nuclei (C_1 and C_2) at high field in a liquid is given by $\mu_H\sigma_z^{(H)} + \mu_C\sigma_z^{(C_1)} + \mu_C\sigma_z^{(C_2)}$, with μ_H and μ_C the nuclear magnetic moments. The standard Pauli matrices are used as an operator basis, and superscripts on operators refer to the nucleus the operator acts on. The cat-state benchmark for this system begins by eliminating signal from the carbon nuclei to obtain the initial state $\sigma_z^{(H)}$. Next, a sequence of quantum gates[18] is used to achieve the state $\sigma_y^{(H)}\sigma_y^{(C_1)}\sigma_z^{(C_2)}$ (Fig. 1), which is a sum of several coherences[19]. In particular, it contains the three coherence $|000\rangle\langle 111| + |111\rangle\langle 000|$, which is the deviation density matrix for the cat state $(|000\rangle + |111\rangle)/\sqrt{2}$ (where

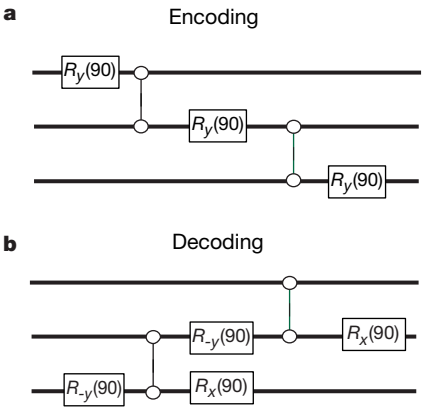

Figure 1 Quantum networks for the cat-state benchmark. **a**, Encoding of the deviation matrix $\sigma_z II$ into $\sigma_y\sigma_y\sigma_x$ by using a cascade of one-qubit rotations ($R_y(90)$) and two-qubit operations (vertical bars) given by *J*-coupling gates. A *J*-coupling gate is given by the unitary operator $e^{-i\sigma_z\sigma_z\pi/4}$. A three coherence $|000\rangle\langle 111| + |111\rangle\langle 000|$ is contained in the output which can be labelled using a magnetic gradient or phase cycling. **b**, Decoding the coherence to a pseudopure state is accomplished by a similar inverse cascade. The output state is $\sigma_x|00\rangle\langle 00|$. Both networks generalize by extending the cascade to more qubits.

0 and 1 represent the 'down' and 'up' states, respectively). If each qubit is rotated by a phase ϕ around the z-axis, the three coherence rotates by 3ϕ, and all other coherences rotate by 0, ϕ or 2ϕ. This can be used to label the three coherence and eliminate all other components of the state, as explained below. After labelling, the three coherence is decoded to the state $\sigma_z^{(H)}|00\rangle\langle 00|$ (Fig. 1) and observed on the proton. The resulting spectrum is compared to a reference spectrum obtained after applying a 90° r.f. pulse to the proton in the initial, thermal state. The reference spectrum has four peaks corresponding to the states $|00\rangle$, $|01\rangle$, $|10\rangle$ and $|11\rangle$ of the carbon nuclei. The spectrum obtained after decoding the cat state should have a single peak, ideally with the same intensity as that of the corresponding peak in the reference spectrum. If errors in the phase labelling method are negligible, as is the case here, then the ratio of these intensities is a lower bound on the average of the fidelities[20] with which the decoding procedure maps the states $|000\rangle \pm \langle 111|$ to the states $(|0\rangle \pm |1\rangle)|00\rangle$.

The three-qubit cat-state benchmark can be generalized to any number n of qubits by repeating the steps of the cascade in the networks shown in Fig. 1. We implemented the seven-qubit version using fully labelled *trans*-crotonic acid (Fig. 2). The qubits are given by the spin-half component of the methyl protons, the two protons adjacent to the double bond and the four ^{13}C nuclei. Figure 3 shows the experimental reference spectrum of C_1 together with the spectrum obtained after decoding. We chose to observe on the methyl carbon because all the couplings are adequately resolved. Errors can show up as peaks in positions different from the leftmost one. We could not detect such errors above the noise. The fidelity of the experiment was measured to be 0.73 ± 0.02.

The success of the experiment derives from the use of the following techniques (described in the Methods): (1) An r.f. selection method to greatly reduce the effects of r.f. inhomogeneities. (2) A gradient-based selection method for removing signal from the spin three-half component of the methyl protons in an almost optimal way. (3) The use of abstract reference frames for each nucleus to absorb chemical shift and first-order off-resonance effects in selective pulses. (4) Precomputation of coupling effects during pulses. (5) A pulse-sequence compiler that optimizes delays between pulses for achieving the desired amount of coupling evolution while minimizing unwanted couplings. All of these techniques are scalable in principle.

	M	H_1	H_2	C_1	C_2	C_3	C_4
M	-969.4						
H_1	6.9	-3560.3					
H_2	-1.7	15.5	-2938.2				
C_1	127.5	3.8	6.2	-2327.0			
C_2	-7.1	156.0	-0.7	41.6	-18599.2		
C_3	6.6	-1.8	162.9	1.6	69.7	-15412.8	
C_4	-0.9	6.5	3.3	7.1	1.4	72.4	-21685.1

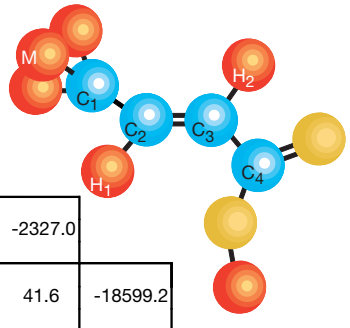

Figure 2 Characteristics of crotonic acid. Molecular structure of *trans*-crotonic acid together with a table of the chemical shifts (on the diagonal) and *J*-coupling constants (below the diagonal). The chemical shifts are given with respect to reference frequencies of 500.13 MHz (protons) and 125.76 MHz (carbons) on the 500 MHz spectrometer we used. The decoherence times (T_2^*) were greater than 2 s.

The cat-state benchmark has three applications that promise to make it useful for NMR and other quantum technologies. First, the ability to implement the cat-state benchmark with high fidelity is a good indication of what types of tasks can be accomplished in the system at hand. In addition, the decoding algorithm of the cat-state benchmark is similar to necessary subroutines of fault-tolerant error-correction[21]. This is a critical issue for scalable quantum information processing, as robustness requires that each operation has a maximum error below some threshold[22–24]. Our experiment involved a total of twelve useful two-qubit operations, so the fidelity of 0.73 suggests an error of about 0.023(=0.27/12) per coupling gate. If this degree of control were available in the context of quantum communication, it would be close to the known thresholds[25].

Second, the output of the benchmark can be used as a reliable pseudopure state for quantum algorithms using one less $(n-1)$ qubit or as the input to an n-bit error-correction benchmark[14]. This requires addressing two problems: the first is to ensure that the labelling method can be used together with a subsequent algorithm, and the second requires that errors accumulated when decoding the n-coherence are eliminated.

The n-coherence can be labelled using gradient methods[19]. This has two drawbacks: they are hampered by diffusion and they are not easily generalizable to other devices. One can instead perform $2n+1$ experiments, where in the kth experiment, the gradient is replaced by explicit pulses that rotate each qubit by a phase $\phi_k = 2\pi k/(2n+1)$. If o_k is the expectation of the observable measured at the end of the kth experiment, then the value $o = \Sigma_k o_k e^{-i2\pi kn/(2n+1)}$ is non-zero only for signal originating at an n-coherence. This technique can be applied in any system where it is possible to apply z-rotations reliably. If the phase of applied pulses is

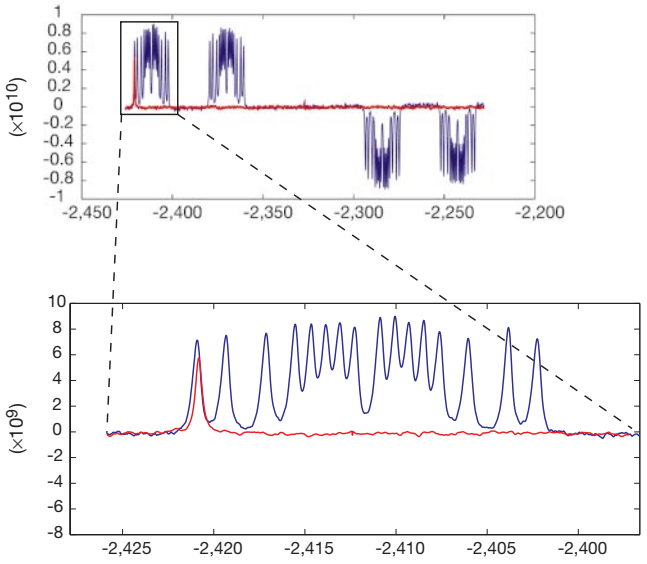

Figure 3 Experimental results: spectra of the pseudopure state (red) and the input state after transfer of polarization to the methyl carbon (blue). The initial steps in the experiments resulting in these spectra were the same, and involved: (1) Signal selection based on radio frequency power. (2) Spin-half selection for the methyl protons. (3) Transfer of polarization to the methyl carbon using one $1/(2J)$ delay. For the pseudopure-state spectrum the next steps were as required for the cat-state benchmark. Both spectra were acquired with 256 scans and are shown at the same scale. The signature of the pseudopure state is that only a single (the leftmost) peak remains. No detectable signal remains in any other peak position. The intensity ratio for the leftmost peak in the pseudopure state and the reference is 0.73 ± 0.02. This compares well to the relative signal of 0.55 measured for the less fragile states accessed in a five-spins system[16] consisting of four nuclear types. The loss of signal is primarily due to spin relaxation, incomplete refocusing of couplings and intrinsic defects in using selective pulses. Horizontal axes, Hz; vertical axes, intensity (arbitrary units).

highly controllable, as in NMR, one can instead change the reference frame for each qubit, which is equivalent to changing the phase of all subsequent pulses and the observation reference phase by $-\phi_k$. This is essentially a phase-cycling method for selecting the n-coherence[26]. We have used both the gradient-based and this phase-cycling method with identical results in the crotonic acid system.

The problem of decoding error can in principle be solved by using the maximum coherence directly as the input for a (modified) algorithm. However, it is not possible to obtain a reference signal for the n-coherence without first mapping it to an accessible observable, which can involve a loss of signal. Furthermore, it may be inconvenient to use the n-coherence instead of the more familiar standard pseudopure state. Our experiments show that we can decode the n-coherence to the pseudopure state with no detectable error in the observed spectrum. Errors in unobserved operators can be eliminated efficiently by performing multiple experiments, each with a random phase of 0° or 180° applied to qubits 2, 3…, a technique which is a special case of the randomized methods of Knill *et al.*[27]. The number of experiments that need to be performed depends on the desired level of suppression of possible error signals. N experiments result in suppression by a factor of $O(1/\sqrt{N})$.

The third application of the cat-state benchmark is to demonstrate the ability to reach the maximum coherence with little loss of signal. Previous experiments have generated coherences by exploiting symmetry and effective hamiltonian methods. Very high order coherences can be observed in the solid state[26]. A maximal coherence of order seven was detected[28] by exploiting symmetry. The methods used in these cases yield only a small fraction of the signal that can be achieved by using methods based on quantum networks.

The realization of the cat-state benchmark given here is in an ensemble setting. Most proposals for quantum devices involve individual systems with pure initial states. In these cases the benchmark can be modified by replacing the ensemble measurements by repetition to infer o_k with sufficiently high signal-to-noise ratio. The preparation step is replaced by a network that directly maps the available initial state to the cat state. We note that any evaluation of a quantum device involves substantial repetition, essentially replacing the ensemble measurement by an ensemble in time. □

Methods

We used a standard 500 MHz NMR spectrometer (DRX-500 Bruker Instruments) with a triple resonance probe to characterize ^{13}C-labelled *trans*-crotonic acid (Fig. 2) at 298K.

To make crotonic acid-1,2,3,4-$^{13}C_4$ we started from ethyl acetoacetate-1,2,3,4-$^{13}C_4$ which was reduced with an excess of sodium borohydride and the alcohol formed was converted to the tosylate in near quantitative yield. The tosylate (unpurified) was then refluxed in ethanol with potassium carbonate to give predominantly the ethyl *trans*-crotonate-1,2,3,4-$^{13}C_4$ (ratio of 97:3 to *cis*). Crotonic acid-1,2,3,4-$^{13}C_4$ was obtained in 91% overall yield by saponification of the ester with aqueous sodium hydroxide in water.

Selective r.f. pulses used in the experiment were designed and analysed by simulation on single and pairs of nuclei and represented optimally as a composition of phase shifts, $\sigma_z\sigma_z$ couplings and an ideal 90° or 180° pulse. The simulation is in principle scalable. This permits elimination of most first-order errors attributable to off-resonance and coupling effects without using specialized shapes.

To implement quantum information processing tasks, we translated an ideal quantum network, expressed in terms of 90° rotations and $1/(2J)$ coupling evolutions, to a pulse sequence. After inserting suitable refocusing pulses, a home-built pulse-sequence compiler optimized the delays between pulses to achieve the desired evolution and minimize errors due to incompletely refocused couplings. Coupling evolutions were calculated based on delays and first-order effects during selective pulses. Optimization involved minimizing the sum of the squares of the predicted coupling over- or under-rotation for each pair of nuclei and step of the quantum network. The final pulse sequence used in our experiment required 48 pulses with a signal loss caused by coupling errors (explicitly estimated by the compiler) of 0.15. Phases for each pulse were with respect to phases of abstract reference frames for each nucleus. The phases of the abstract reference frames were precomputed based on chemical shift evolution and first-order side-effects caused by selective pulses.

The effect of pulse imperfections due to r.f. inhomogeneities was reduced by selecting signal based on r.f. power. The method exploits the dependence of the nutation rate on r.f. power and is similar to previously implemented r.f. imaging methods[29]. Our implementation consisted of the following sequence applied to the methyl protons: $90^\circ_x - (180^\circ_{-x})^{64} - (180^\circ_{\phi_i} - 180^\circ_{-\phi_i})^{64} - 90^\circ_y$. The phases ϕ_i were modulated by a 64-point gaussian. The sum of these angles was 22.5°. To remove unwanted signal, each experiment was repeated twice, with the selection sequence in the second experiment using $-\phi_i$ instead of ϕ_i. The signals from the two experiments were subtracted. The signal selected by this sequence is r.f.-homogeneous to within ±2%. By calibrating the power, we were able to retain about 25% of the signal compared to an unselected spectrum. This sequence also selects signal from only the methyl protons so that the initial state is $\sigma_z^{(M)}$.

To use the three methyl protons as a single effective spin-half particle, we exploited the fact that, owing to symmetry, the state space of the protons consists of one spin three-half component and two spin-half components. The initial state involves polarization in both spin types. It suffices to eliminate signal from the first while retaining polarization from the second. This was accomplished by using a three-step sequence involving transfer of polarization to the adjacent carbon and terminated by a gradient 'crusher' (details available from the authors). The elimination of signal from the spin three-half states was verified by observing the signal on the adjacent carbon after transfer of the methyl polarization with different coupling delays. Signal from the spin three-half component shows up in the extreme pair of the four main peaks given by the coupling to the methyl protons. We were unable to detect any error signal above the noise.

The remaining steps of the experiment consist of generation and labelling of the n-coherence, and decoding operations to obtain the standard pseudopure state. The sequence is as described, with inserted refocusing pulses and optimized delays. Knowledge of the intended current state of a nucleus was used when that state was $|0\rangle\langle 0|$ or $|1\rangle\langle 1|$, to absorb the effects of couplings to that nucleus in the reference frame[30].

Received 30 August 1999; accepted 27 January 2000.

1. Simon, D. R. On the power of quantum computation. *SIAM J. Comput.* **26,** 1474–1483 (1997).
2. Shor, P. W. Polynomial-time algorithms for prime factorization and discrete logarithms on a quantum computer. *SIAM J. Comput.* **26,** 1484–1509 (1997).
3. Wiesner, S. Conjugate coding. *Sigact News* **15,** 78–88 (1983).
4. Bennett, C., Bessette, F., Brassard, G., Salvail, L. & Smolin, J. Experimental quantum cryptography. *J. Cryptol.* **5,** 3–28 (1992).
5. Cirac, J. & Zoller, P. Quantum computations with cold trapped ions. *Phys. Rev. Lett.* **74,** 4091–4094 (1995).
6. Loss, D. & DiVincenzo, D. P. Quantum computation with quantum dots. *Phys. Rev. A* **57,** 120–126 (1997).
7. Bocko, M. F., Herr, A. M. & Feldman, M. J. Prospects for quantum coherent computation using superconducting electronics. *IEEE Trans. Appl. Supercond.* **7,** 3638–3641 (1997).
8. Shnirman, A., Schön, G. & Hermon, Z. Quantum manipulations of small josephson junctions. *Phys. Rev. Lett.* **79,** 2371–2374 (1997).
9. Cory, D. G., Fahmy, A. F. & Havel, T. F. Ensemble quantum computing by nmr-spectroscopy. *Proc. Natl Acad. Sci. USA* **94,** 1634–1639 (1997).
10. Gershenfeld, N. A. & Chuang, I. L. Bulk spin resonance quantum computation. *Science* **275,** 350–356 (1997).
11. Kane, B. E. A silicon-based nuclear spin quantum computer. *Nature* **393,** 133–137 (1998).
12. Jones, J. A., Mosca, M. & Hansen, R. H. Implementation of a quantum search algorithm on a quantum computer. *Nature* **392,** 344–346 (1998).
13. Chuang, I. L., Vandersypen, L. M. K., Zhou, X., Leung, D. W. & Lloyd, S. Experimental realization of a quantum algorithm. *Nature* **393,** 143–146 (1998).
14. Cory, D. G. *et al.* Experimental quantum error correction. *Phys. Rev. Lett.* **81**, 2152–2155 (1998).
15. Nielsen, M. A., Knill, E. & Laflamme, R. Complete quantum teleportation. *Nature* **396,** 52–55 (1998).
16. Marx, R., Fahmy, A. F., Myers, J. M., Bermel, W. & Glaser, S. J. Realization of a 5-bit nmr quantum computer using a new molecular architecture. Preprint quant-ph/9905087 at ⟨http://xxx.lanl.gov⟩ (1999).
17. Sörensen, O. W., Eich, G. W., Levitt, M. H., Bodenhausen, G. & Ernst, R. R. Product operator-formalism for the description of nmr pulse experiments. *Prog. Nucl. Magn. Reson. Spectrosc.* **16** (1983).
18. Barenco, A. *et al.* Elementary gates for quantum computation. *Phys. Rev. A* **52**, 3457–3467 (1995).
19. Freeman, R. *Spin Choreography* (Oxford Univ. Press, 1998).
20. Schumacher, B. Sending entanglement through noisy quantum channels. *Phys. Rev. A* **54,** 2614–2628 (1996).
21. Shor, P. W. in *Proc. Symp. Foundations of Computer Science* 56–65 (IEEE, Los Alamitos, California, 1996).
22. Aharonov, D. & Ben-Or, M. in *Proc. 29th Ann. ACM Symp. Theory of Computing* 176–188 (Association for Computing Machinery, New York, 1996).
23. Kitaev, A. Y. Quantum computations: algorithms and error correction. *Uspekhi Mat. Nauk.* **52,** 53–112 (1997).
24. Knill, E., Laflamme, R. & Zurek, W. H. Resilient quantum computation. *Science* **279,** 342–345 (1998).
25. Dür, W., Briegel, H.-J., Cirac, J. I. & Zoller, P. Quantum repeaters for based on entanglement purification. *Phys. Rev. A* **59,** 169–181 (1999).
26. Emsley, L. & Pines, A. in *Proc. Int. School of Physics, Enrico Fermi* Vol. CXXIII, 123–266 (North-Holland, Amsterdam, 1994).
27. Knill, E., Chuang, I. & Laflamme, R. Effective pure states for bulk quantum computation. *Phys. Rev. A* **57,** 3348–3363 (1998).
28. Weitekamp, D. P., Garbow, J. R. & Pines, A. Determination of dipole coupling constants using heteronuclear multiple quantum nmr. *J. Chem. Phys.* **77,** 2870–2883 (1982).
29. Maffei, P., Elbayed, K., Brondeau, J. & Canet, D. Slice selection in nmr imaging by use of the b1 gradient along the axial direction of a saddle-shaped coil. *J. Magn. Reson.* **95,** 382–386 (1991).
30. Vandersypen, L. M. K., Yannoni, C. S., Sherwood, M. H. & Chuang, I. L. Realization of logically labeled effective pure states for bulk quantum computation. *Phys. Rev. Lett.* **83,** 3085–3088 (1999).

Acknowledgements

We thank D. Cory, G. Fernandez, T. Havel, S. Lacelle, D. Lemaster, D. Meyer, C. Unkefer, A. M. Wang and W. H. Zurek for help and discussions.

Correspondence and requests for materials should be sent to E.K. (e-mail: knill@lanl.gov).